# A New Approach to Pruning Volterra Models for Power Amplifiers

Carlos Crespo-Cadenas*, *Member, IEEE,* Javier Reina-Tosina, *Member, IEEE,*
María J. Madero-Ayora, *Member, IEEE,* and Jesús Muñoz-Cruzado
EDICS: NSP-NSID Nonlinear system identification; linearization

***Abstract*—The objective of this paper is to present an approach to behavioral modeling that can be applied to predict the nonlinear response of power amplifiers with memory. Starting with the discrete-time, complex-baseband full Volterra model, we define a novel methodology that retains only radial branches that can be implemented with one-dimensional finite impulse response filters. This model is subsequently simplified by selecting a subset of directions using an ad-hoc procedure. Both models are evaluated in terms of accuracy in the time and frequency domains and complexity, and are compared with other models described in the literature. The evaluation is conducted using a low-voltage silicon RF driver amplifier and a 5-W PA, which are characterized at different levels with diverse modulation formats, including wideband code-division multiple access (WCDMA) and orthogonal frequency-division multiplexed (OFDM) signals. In all cases, comparison of the measured and simulated responses confirms the effectiveness of the proposed approach.**

***Index Terms*—Dynamic behavioral models, memory polynomials, nonlinear identification, power amplifiers, Volterra series.**

## I. Introduction

MODERN wireless communication systems are designed to operate with signals that have large bandwidth and high peak-to-average ratio (PAR). Important nonlinear effects are generated in the power amplifier (PA) by the envelope variations of these signals, spectral regrowth being one of the most significant. For that reason, special efforts have been invested in order to attain a deeper knowledge of the nonlinear behavior of these systems.

One of the most successful techniques devoted to the study of PAs is the Volterra series, involving kernels that contain all the information for a nonlinear system with fading memory. The domain of an $n$th–order Volterra kernel can be visualized as a discrete grid forming an $n$–dimensional ($n$–D) hypercube. The use of these kernels implies a computationally expensive multidimensional filtering of the input envelope, which can be pruned by realizing a lower number of one-dimensional (1–D) filters. Different criteria have been proposed in several published papers to obtain this reduction, as discussed below.



This work was supported by the Spanish National Board of Scientific and Technological Research (CICYT) under Project TEC2008-06259/TEC, and by the Regional Government of Andalusia (CICE) under Grant P07-TIC-02649.

The authors are with the Departamento de Teoría de la Señal y Comunicaciones, Escuela Superior de Ingenieros, Universidad de Sevilla, Spain. Tel: +34954487336, Fax: +34 954487341. E-mail: ccrespo@us.es, jreina@us.es, mjmadero@us.es, jmcalba@us.es.

For example, the parallel Hammerstein or *memory polynomial* (MP) model [1] uses only one branch for each order with 1–D filters (one-dimensional convolutions) involving the coefficients lying along the main diagonal of each $n$–D hypercube.

In [2], a pruning approach was presented in which the structure accepts nearly diagonal terms, and those coefficients that are far away from the main diagonal are removed. In that technique, an index is introduced to adjust the complexity reduction according to the needed accuracy. Reported results show a low normalized mean-square error (NMSE) for a fifth-order model identified with a parameter called the "near-diagonality" coefficient by the authors of [2]. Related to this method are other efficient model-pruning approaches to Volterra structures [3].

A review of the most advanced models was presented in [4], which also introduced a new structure formed with the MP structure combined with cross terms between the signal and lagging and/or leading exponentiated envelope terms, which is referred to as the *generalized memory polynomial* (GMP) model.

Other discrete-time complex envelope models based on *a priori* knowledge of the PA circuit model have been recently presented [5], [6], [7]. In [5], the authors propose a model for wideband amplifiers deduced under the assumption of transfer functions with a flat response in all harmonic zones except at dc where the (even) nonlinear transfer functions cannot be considered flat, because of low-frequency dispersive effects and load impedance dependence on baseband frequency. This *Volterra behavioral model for wideband amplifiers* (VBW), presents a distinct "off-diagonal" structure. In [6], a behavioral power amplifier model is also derived starting from previous knowledge about the amplifier, and the authors claim an NMSE substantially lower than for the well-known and widely used MP model. The two models, VBW and [6], present a similarity in the fact that filtering involves samples of the instantaneous power. Although in the case of the VBW no filtering is applied to the complex-envelope samples, the fidelity of this model is remarkably better than the MP. This property is also realized in the *envelope-memory polynomial* model [8], which can be easily derived from the VBW as a particular case. This structure has also been valued as advantageous for the design of digital predistorters.

An extended version of the VBW model and its efficiency are analyzed in [9], where an equivalent discrete-time baseband PA model considering memory effects and bandpass

nonlinearity is formulated by joining the MP and VBW approaches. The accuracy of the so-called *extended* VBW (EVBW) model is reflected in significantly lower NMSE than for the MP model and similar to [6], which contains a larger number of coefficients.

The structural proposals shown in the present work are based on an underlying general Volterra model of the PA. The introduced perspective relies on a novel pruning approach involving 1–D filters, by following selected radial directions that emanate from the origin of the hypercubes. As a consequence of this radial pruning, the resulting structures exhibit good prediction performance, notwithstanding the reduction of model coefficients compared not only to the full Volterra (FV) model, but also to the most efficient models published recently.

The paper is organized as follows. After this introduction, we first present general remarks about Volterra models in order to introduce the notation that will be used. Section II also contains a detailed description of the proposed pruning methodology, starting with third-order kernels in Section II-A and generalizing the approach to the $n$th-order kernel in Section II-B. The complete representation will be referred to as the *radially pruned Volterra* (RPV) model. Section II-C discusses a further reduction of this structure and introduces the *simplified* RPV (SRPV) model. Finally, Section II-D comments on the underlying radial structure corresponding to the VBW and EVBW models. In Section III, the computational complexity of the aforementioned models is examined and is compared to other widely used approaches. Sections IV and V compare the performance of the radially pruned models with other efficient models, employing measurement data from two real amplifiers driven with wideband code-division multiple access (WCDMA) and orthogonal frequency-division multiplexed (OFDM) signals, respectively. Finally, some concluding remarks are outlined in Section VI.

## II. Radially Pruned Models

Let $x(k)$ denote complex-envelope samples of the RF input signal driving a nonlinear amplifier of a wireless communications system. The amplifier can be described by a discrete-time finite-memory complex baseband Volterra model, whose output complex envelope $y(k)$ can be written as

$$y(k) = \sum_{\substack{n=1 \\ n-\text{odd}}}^{N} \sum_{\mathbf{q}_n=\mathbf{0}}^{\mathbf{Q}_n} h_n(\mathbf{q}_n) x(k-q_1) \times \\ \times \prod_{m=1}^{(n-1)/2} x(k-q_{2m}) x^*(k-q_{2m+1}), \quad (1)$$

where the first summation is restricted to odd values of $n$, $h_n(\mathbf{q}_n)$ represents the discrete-time Volterra kernels of order $n$ and $\mathbf{q}_n$ is an $n$–dimensional vector composed of the integer-valued delays, $q_i = 0, \cdots, Q_n$ for all $i$. Here we consider decaying memory with the same finite length $Q_n = Q$, for all odd orders $n = 1,\ 3, \cdots, N$. In the following, we will denote the set of $n$th-order Volterra regressors as $\Pi_n\{x(k), \mathbf{q}_n\}$ ($n$ odd), defined as $\Pi_1\{x(k), q_1\} = x(k-q_1)$ and

$$\Pi_n\{x(k), \mathbf{q}_n\} = x(k-q_1) \prod_{m=1}^{(n-1)/2} x(k-q_{2m}) x^*(k-q_{2m+1}), \quad (2)$$

for $n \geq 3$. It is opportune to view the Volterra model (1) as a special case of a linear regression model [10].

The full Volterra model (1) is equivalent to a filter bank that involves a huge number of coefficients, growing exponentially with the filter order $n$ and the maximum delay $Q$. Several approaches discussed in the introduction allow us to devise each $n$th-order term as the contribution of a limited number of 1–D finite-impulse response (FIR) filters, with the total number of coefficients increasing linearly with $Q$, a desirable feature. However, all these approximations to the FV model are of limited accuracy. That is the case of the MP model, which is arranged with coefficients laid along the main diagonal of the corresponding kernel. The same basic idea can be applied to sort out definite directions in the delay space, each requiring a 1–D FIR filter, but selecting these directions with a different criterion in order to build a pruned model with higher accuracy. Since a finite fading-in-time memory has been assumed, the importance of the coefficients will diminish as their temporal position moves away from the origin. In that case, it seems reasonable to selectively retain only the most relevant terms, i.e., those in the neighborhood of the memoryless term $h_n(\mathbf{0})$ in each radial direction. Using set notation, we will refer to the following subset of Volterra regressors:

$$\Pi_{n,r,s}\{x(k), q\} = \Big\{ \Pi_n\{x(k), \mathbf{q}_n\} \ \Big| \ q_i \text{ define the radial direction } s \text{ of type } r \Big\}, \quad (3)$$

where $r$ indicates the type of radial direction and $s$ is the particular branch belonging to $r$. Note that the MP and the VBW models are consistent with this property, because the main diagonal and the filtering of the VBW involve radial directions. For example, the set of regressors for the third-order kernel of the MP model can be defined as:

$$\Pi_{3,3,1}\{x(k), q\} = \Big\{ \Pi_3\{x(k), \mathbf{q}_3\} \ \Big| \ q_i = q\,, \forall\ i = 1,2,3 \Big\}. \quad (4)$$

In this case, there is only one branch ($s = 1$) belonging to the main diagonal direction ($r = 3$). Similarly, in the case of the VBW model, the set of regressors for the third-order kernel can be expressed with the set notation as:

$$\Pi_{3,2,2}\{x(k), q\} = \Big\{ \Pi_3\{x(k), \mathbf{q}_3\} \ \Big| \ q_i = 0\,, i = 1,2,3, \text{ and } q_j = q\,, \forall\ j \neq i \Big\}. \quad (5)$$

Here, the radial direction is labeled $r = 2$ with two branches belonging to this direction. This notation is discussed in more detail in the next subsections.

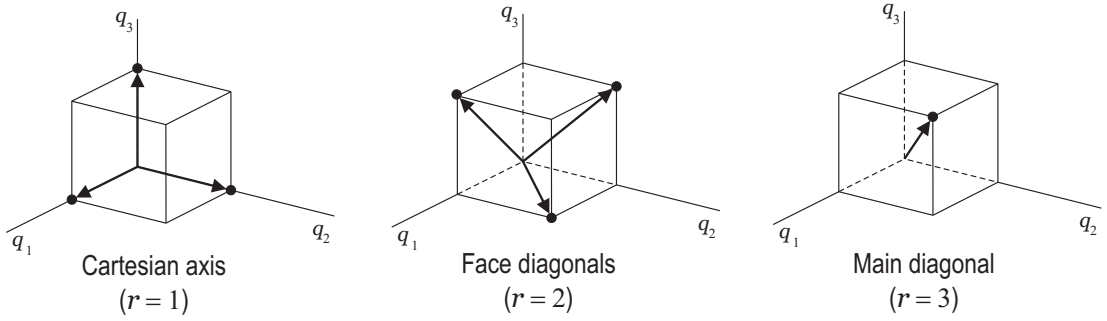


Fig. 1. Lattice of the third-order kernel domain.

### A. Third-Order Kernel

To illustrate the idea concerning this radial pruning, let us begin by analyzing the simple case of a third-order kernel. Consider a PA with the unit-delay ($Q = 1$) third-order kernel $h_3(\mathbf{q}_3)$, represented in Fig. 1. We designate the types of radial directions as: $r = 1$ for the 3–D Cartesian axis, $r = 2$ for the diagonals of each cube face, emerging from the origin, and $r = 3$ for the main diagonal. Let $S_{3,r}$ be the number of radial directions of type $r$. Therefore, any radial direction can be denoted by $\Pi_{3,r,s}$, where $s = 1, \cdots S_{3,r}$. Symmetry reasons restrict $S_{3,r} = 2$ for $r = 1, 2$ (Cartesian axis and face diagonals, respectively), and $S_{3,3} = 1$ (main diagonal). The regressors associated with the radial directions are:

- The Cartesian axis directions: The direction of the $i$th axis ($i = 1, 2, 3$) is defined by $q_i = q$ and $q_j = 0$ for all $j \neq i$. Then, each one of the two types of regressors ($S_{3,1} = 2$) is given by

$$\Pi_{3,1,1}\{x(k), q\} = x^2(k)x^*(k-q)$$

and

$$\Pi_{3,1,2}\{x(k), q\} = |x(k)|^2 x(k-q).$$

- Diagonals of the cube faces: The $i$th face ($i = 1, 2, 3$) containing the origin of the cube is mathematically defined in the delay space by $q_i = 0$, and the direction of its diagonal by $q_j = q$ ($j \neq i$). In this case, there are also two types of regressors ($S_{3,2} = 2$) with expressions

$$\Pi_{3,2,1}\{x(k), q\} = x^2(k-q)x^*(k)$$

and

$$\Pi_{3,2,2}\{x(k), q\} = |x(k-q)|^2 x(k).$$

- Main diagonal, $q_i = q$ for $i = 1, 2, 3$: Only one diagonal direction is possible ($S_{3,3} = 1$) and its regressors are

$$\Pi_{3,3,1}\{x(k), q\} = |x(k-q)|^2 x(k-q).$$

Note that all these regressors depend on a single, scalar delay ($q$), as they are associated to 1–D filters. It is worthwhile to note that $\Pi_{3,3,1}\{x(k), q\}$ and $\Pi_{3,2,2}\{x(k), q\}$ are regressors of the MP and VBW models, respectively, as commented above.

From this, we can replace the 3–D filtering with an equivalent structure composed of five 1–D filters. Since $Q = 1$, the new filter-bank has the same number of coefficients as the general Volterra third-order model (i.e., no pruning has been applied to the 3–D filter). Filtering being limited to these five 1–D convolutions, the pruning starts to be effective as $Q$ increases. If such is the case, the number of coefficients will grow linearly, not exponentially, with corresponding complexity reduction.

### B. Radial Pruning of an $n$th-Order Kernel

A general Volterra kernel can be represented by a grid forming an $n$–D cube (hypercube) and selection of the radial directions can be performed in a way similar to that followed with the third-order kernel. In that case, the first two filters are constructed with the coefficients of the Cartesian axis, the second two filters use those in the diagonals of the cube faces, and the remaining filter is formed with coefficients belonging to the main diagonal. Denoting by $S_{n,r}$ the number of radial directions of type $r$ for the case of an $n$th-order kernel, and following a similar procedure (i.e., upgrading the dimensionality from the Cartesian axis to the main diagonal), the adopted regressors for the 1–D FIR filters are

- Cartesian axis directions: The direction of the $i$th axis ($i = 1, 2, \ldots, n$) is defined by $q_i = q$ and $q_j = 0$ ($j \neq i$). In this case, there are $S_{n,1} = 2$ types of regressors, expressed as

$$\Pi_{n,1,1}\{x(k), q\} = x^2(k)|x(k)|^{n-3}x^*(k-q)$$

and

$$\Pi_{n,1,2}\{x(k), q\} = |x(k)|^{n-1}x(k-q).$$

- Diagonals of the $(n-2)$-D hyper-planes: The $i$th $(n-2)$-D facet ($i = 1, 2, \cdots, n$) of the hypercube in the delay space is mathematically defined by $q_{i'} = q_i = 0$ ($i' \neq i$) and the direction of its diagonal by $q_j = q$, for all $j \neq i, i'$. According to (2), there are $S_{n,n-2} = 3$ types of regressors given by

$$\Pi_{n,n-2,1}\{x(k), q\} = |x(k-q)|^{n-3}x^2(k)x^*(k-q),$$

$$\Pi_{n,n-2,2}\{x(k), q\} = |x(k-q)|^{n-3}|x(k)|^2 x(k-q)$$

and

$$\Pi_{n,n-2,3}\{x(k), q\} = |x(k-q)|^{n-5}x^3(k-q)x^{*2}(k).$$

The diagonals of the hyper-planes of different dimensions can be defined in a similar way:

- Diagonals of the $(n-1)$-D hyper-facets: The $i$th $(n-1)$-D facet ($i = 1, 2, \cdots, n$) of the hypercube is defined by

$q_i = 0$ and the direction of its diagonal by $q_j = q$, for all $j \neq i$. The expressions for the $S_{n,n-1} = 2$ types of regressors are

$$\Pi_{n,n-1,1}\{x(k), q\} = |x(k-q)|^{n-3} x^2(k-q) x^*(k)$$

and

$$\Pi_{n,n-1,2}\{x(k), q\} = |x(k-q)|^{n-1} x(k).$$

- Main diagonal, $q_i = q$ for $i = 1, 2, \cdots, n$: The regressor on the main diagonal ($S_{n,n} = 1$) is

$$\Pi_{n,n,1}\{x(k), q\} = |x(k-q)|^{n-1} x(k-q).$$

The model obtained after selection of these radial directions, which we call a radially pruned Volterra (RPV) model, can be expressed by the following equation

$$y_{\text{RPV}}(k) = \sum_{n=1}^{N} \sum_{r=1}^{n} \sum_{s=1}^{S_{n,r}} \sum_{q=0}^{Q} h_{n,r,s}(q) \Pi_{n,r,s}\{x(k), q\}. \quad (6)$$

The RPV model contains a finite number of radial directions, given by single, scalar delay ($q$) regressors, or 1–D FIR filters with $Q$ coefficients each. For that reason, the complexity grows linearly with $Q$ instead of the exponential growth of the FV model [11], as discussed in the following section.

### C. Simplified Model with Radial Pruning

According to the preceding discussion, the radial pruning of a Volterra model yields a novel structure, the RPV model with a reduced number of coefficients. In some cases, the trade-off between accuracy and computational cost makes it desirable to give up part of the model precision in order to further reduce its complexity. This can be achieved with a second step in the pruning process, consisting of the removal of some of the less relevant 1–D convolutions. In agreement with previous remarks, the third-order Volterra filter is approximated with 1–D filtering in five radial directions, whereas in an $n$th-order Volterra term with $n > 3$, the number of radial directions increases. Likewise, we propose a new pruned structure for the $n$th-order Volterra filter, limited to the five radial directions of the third-order kernel, and call this the simplified RPV (SRPV) model.

We have also adopted a more user-friendly notation for the regressors $\Pi_{n,r}\{x(k), q\}$, with only two indexes indicating the order $n$, and the direction $r = 1, \cdots, 5$. The regressors are:

- Main diagonal

$$\Pi_{n,1}\{x(k), q\} = |x(k-q)|^{n-1} x(k-q).$$

- Diagonals of the $(n-1)$-D hyper-facets: There are two types of regressors given by

$$\Pi_{n,2}\{x(k), q\} = |x(k-q)|^{n-3} x^2(k-q) x^*(k)$$

and

$$\Pi_{n,3}\{x(k), q\} = |x(k-q)|^{n-1} x(k).$$

- Cartesian axis directions: The regressors are

$$\Pi_{n,4}\{x(k), q\} = x^2(k) |x(k)|^{n-3} x^*(k-q)$$

and

$$\Pi_{n,5}\{x(k), q\} = |x(k)|^{n-1} x(k-q).$$

The output of the SRPV model can be expressed by the following equation

$$y_{\text{SRPV}}(k) = \sum_{n=1}^{N} \sum_{r=1}^{5} \sum_{q=0}^{Q} h_{n,r}(q) \Pi_{n,r}\{x(k), q\}. \quad (7)$$

### D. Other Models with Radial Structure

To complete the proposal of radial pruning, let us mention other models with simplified radial structure that have been recently published. Firstly, the Hammerstein model and its generalization, the MP model, have diagonal structures in accordance with the radial selection proposed in this paper. Another structure that has provided some helpful clues in the pruning of the FV behavioral model is the VBW model [5]. This behavioral model for wideband amplifiers was formally derived starting from the equivalent circuit and following a conventional Volterra analysis, and also presents 1–D filtering in radial directions. Finally, the EVBW model [9] is formulated by joining the MP and the VBW approaches.

## III. Complexity of the Proposed Models

An important issue in the expression of a behavioral model is the number of coefficients, both at the identification phase and for the prediction of the PA output response. In the proposed RPV model, a major requirement is to gain a significant computational reduction compared to the FV model, for which the complexity has been analysed in [11]. As other published approaches, the RPV model has the advantage that the pruning methodology is based on retaining only a few directions of the delay space, yielding a reduced number of 1–D filters. For an RPV model truncated to order $N = 2P + 1$, the number of coefficients can be expressed as:

$$M = (P+1)(Q+1) + (3+P)PQ\,. \quad (8)$$

This equation shows that the RPV model exhibits a linear increment of the number of coefficients with respect to $Q$, instead of the exponential increase of the FV model.

Regarding the SRPV model, as only five branches are retained, it can be implemented with an even more reduced set of 1-D filters. The number of terms is expressed in closed form as:

$$M = (P+1)(Q+1) + 4PQ\,. \quad (9)$$

It is worthwhile noting that the number of coefficients in the SRPV model shows a linear dependence on $Q$, like the RPV does, and also a linear dependence with respect to the model order, $N = 2P + 1$.

A comparison of the different models in terms of complexity is shown in Fig. 2, where the number of coefficients has been represented versus the maximum delay $Q$ for different fifth-order models. The extreme cases are the FV model (dotted line), with an exorbitant number of coefficients, and the MP model (dot-dashed line and upward triangles), with a modest linear dependence. Slightly more complex than the MP, and

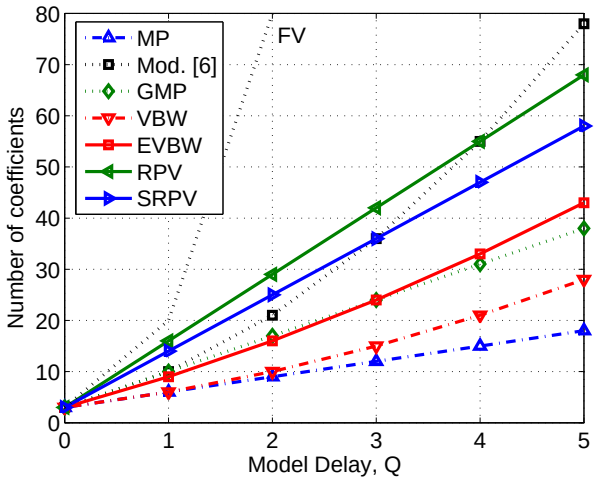


Fig. 2. Number of coefficients for different fifth-order behavioral models.

exhibiting an exponential dependence, is the VBW model (dot-dashed and downward triangles). The model of [6] presents the same dependence, but with a significant increase in the number of parameters. The RPV model (continuous line and left-pointed triangles) has moderate complexity, and thanks to its linear behavior, the number of coefficients is maintained below that of the model of [6] for $Q \geq 4$. The EVBW (continuous line and squares) and GMP (dotted line and diamonds) models display approximately similar performance, with a slight reduction of GMP complexity for $Q \geq 4$. It is evident that although the number of coefficients in EVBW rises exponentially with $Q$, this number is specially reduced and highly competitive. Finally, the SRPV model (continuous line and right-pointed triangles) displays intermediate values between the GMP and the RPV models. According to this figure, we can classify the models into three groups in relation to the computational cost for a given maximum delay. For example, in the case of $Q \geq 4$, the RPV model and the model of [6] are computationally more expensive, the GMP model and the EVBW model have a moderate complexity, and finally the VBW is in the least expensive range. As we will demonstrate in the following section, the SRPV appears as a compromise to avoid the high computational cost of RPV, yet maintaining acceptable accuracy.

Although even-order terms can be considered in the base-band representation [12], we have excluded them from all models in this study, because there are no even-order terms in the bandpass PA model, and it is the aim of this paper to preserve a tight relation between the baseband approach and the bandpass Volterra model. However, the possibility exists of including these even terms to enhance the basis set, thus reducing the modeling error.

## IV. Application to a Real RF Amplifier

For the evaluation of the presented model, we have used a commercial amplifier. The evaluation board was designed using a MAX2430 surface-mount packaged device (MAXIM Integrated Products Inc., Sunnyvale, CA), which is a low-voltage silicon RF PA operating in the frequency range of 800-1000 MHz, suitable as a driver amplifier for portable and mobile telephone systems. Measurements were performed at 915 MHz using the manufacturer's commercially available evaluation board, with the device operating as a class-AB amplifier by applying the recommended bias voltage of 3.6 V. The experimental setup has been presented elsewhere [5].

The initial characterization of the model is performed by evaluating its ability to predict the PA output waveform. The first probing signal was a WCDMA-like signal with a bandwidth of 2 MHz, a PAR of 4.5 dB, and at levels of $-14$ dBm, $-12$ dBm, and $-10$ dBm. With these signal levels, the amplifier is operating in the nonlinear regime with a peak power beyond $-11$ dBm, the 1-dB compression point. The coefficients of a fifth-order model were extracted by using the measured output waveform (sampled at a rate of 10 Msa/s) via a conventional least-squares algorithm [4],[13], and the NMSE with respect to the measured signal was calculated with the RPV model for different maximum delays. According to the complexity shown in Fig. 2, it is possible to map $Q$ to the number of coefficients in order to provide a common reference to compare the different models. The results of the RPV and SRPV models are presented in Fig. 3 by a solid line (left-pointed and right-pointed triangles, respectively). The same figure also shows the performance of the other relevant models under study.

According to this figure, the proposed RPV model obtains the lowest NMSE when the number of coefficients is above or equal to 29 (corresponding to $Q = 2$ for this model), and this fact is more noticeable as the amplifier is operated in a more nonlinear condition. The identification test in Fig. 3(c) for $P_i = -10$ dBm shows that the RPV model obtains an NMSE that improves [6] by 1 dB, although the latter is more complex.

Accepting the restriction of equal complexity, the RPV and SRPV models compare favorably with respect to the other approaches in the full range of complexities. Another way of interpreting this figure is to compare the NMSE for the same maximum delay. For example with $Q = 1$, there is an improvement of over 3 dB with the RPV model against the MP model in Fig. 3(a).

Using the identified fifth-order kernels of Fig. 3(c), the responses with the validation set of WCDMA signals (PAR $= 4$ dB) are plotted in Fig. 4 in terms of the NMSE. The figure shows an almost similar validation performance of all the models with an NMSE of approximately $-34$ dB, against identification values ranging from $-37$ to $-35$ dB. We observe that for a number of coefficients above 24, there is a degradation of a few tenths of dB in the characteristic of GMP, and the same applies to [6] when the number of coefficients is greater than 36.

## V. Model Performance with OFDM Signals

The models described in the preceding sections have also been tested with OFDM signals, in correspondence with the growing trend to include multicarrier modulations in the physical layers of today's wireless communications standards. The applied probing signal was designed to meet a 2-MHz

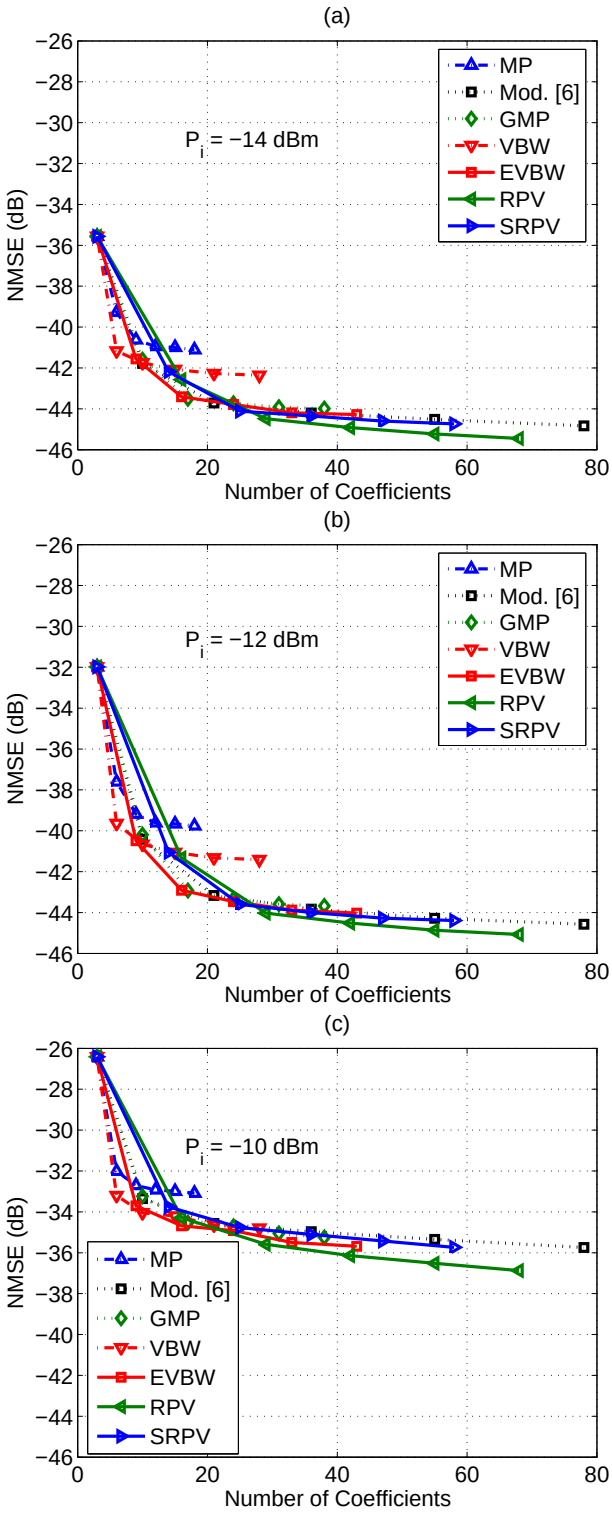


Fig. 3. Comparison of fifth-order models in terms of the NMSE as a function of the number of coefficients. The marks correspond to maximum delays in the range from 0 to 5 samples. Amplifier under test: MAX2430 driven by a 915-MHz WCDMA signal with 4.5-dB PAR. (a) Input level of −14 dBm. (b) Input level of −12 dBm. (c) Input level of −10 dBm.

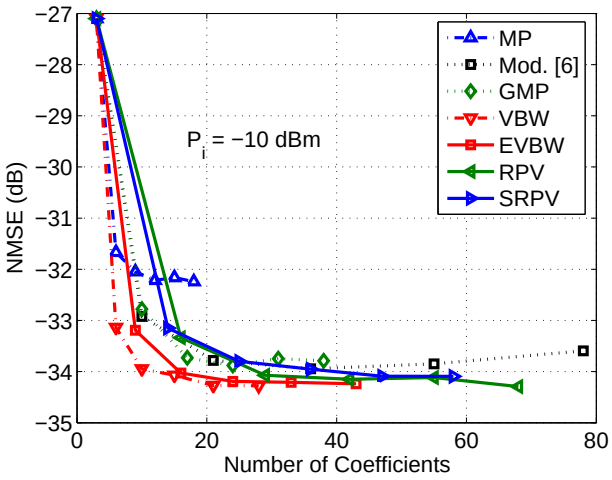


Fig. 4. Performance of the different fifth-order models in terms of the NMSE as a function of of the number of coefficients. The marks correspond to maximum delays in the range from 0 to 5 samples. Amplifier under test: MAX2430. Model identification of Fig. 3(c) was used (−10 dBm), and validation was accomplished by using a different test WCDMA signal with 4-dB PAR.

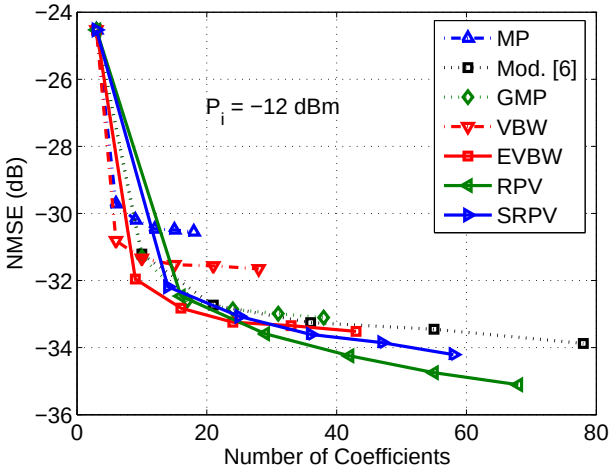


Fig. 5. Comparison of fifth-order models in terms of the NMSE as a function of the number of coefficients. The marks correspond to maximum delays in the range from 0 to 5 samples. Amplifier under test: MAX2430 driven with a 915-MHz OFDM signal with 8 subcarriers and 8.4-dB PAR at a level of −12 dBm.

bandwidth with a mean power level of −12 dBm, and uses eight subcarriers. The OFDM symbols were pre-processed with a root-raised cosine filter using a roll-off factor of 0.25 and a delay of 24 symbols, yielding a PAR of 8.4 dB.

The NMSE values associated with each of the fifth-order models are shown in Fig. 5. The amplifier under test was the MAX2430 device biased as a class-AB amplifier. Although the excitation signal drove the amplifier into a clearly nonlinear regime, it is evident that the RPV model obtains the best overall performance in all cases. With a complexity equal or higher than 29 coefficients (i.e., $Q \geq 2$ for RPV and $Q \geq 3$ for SRPV), the proposed models offer NMSE improvements in the range of 1–2 dB over the model in [6]. It is also notable

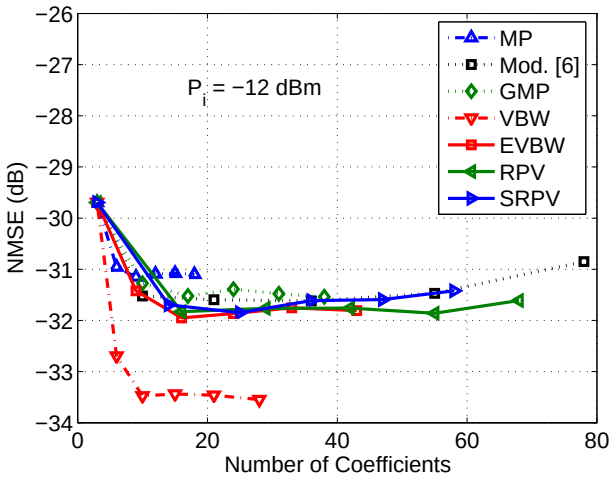


Fig. 6. Cross-validation of the different fifth-order models in terms of the NMSE as a function of the number of coefficients. The marks correspond to maximum delays in the range from 0 to 5 samples. Amplifier under test: MAX2430 driven with a 915-MHz WCDMA signal at a level of −12 dBm and 4-dB PAR. Model identification was accomplished by using a 915-MHz OFDM test signal with 8 subcarriers and 8.4-dB PAR at the same level.

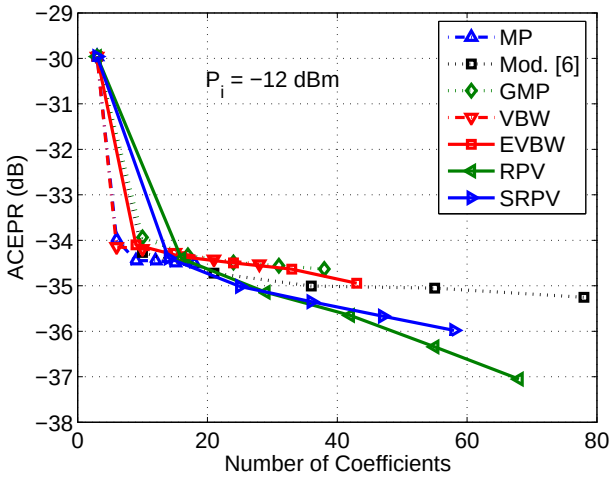


Fig. 7. Comparison of fifth-order models in terms of the ACEPR as a function of the number of coefficients. The marks correspond to maximum delays in the range from 0 to 5 samples. Amplifier under test: MAX2430 excited by a 915-MHz OFDM signal with 8 subcarriers and 8.4-dB PAR at a level of −12 dBm.

that even though EVBW is similar to the GMP model in terms of computational cost, its performance is slightly better.

A further step is the cross-validation of the models by using different signal waveforms to extract model coefficients and to assess model accuracy. For this purpose, the OFDM probing set applied in Fig. 5 is again used for model identification, and the parameter values so obtained are employed to predict the output response of the PA driven by a WCDMA-like signal. We remark that these are very different types of signals, with a difference in the peak-to-average power ratios above 3 dB. The NMSE values of the modeled outputs are depicted in Fig. 6 in terms of the number of coefficients for the different models. These results were obtained carrying out the identification and validation tests on the same evaluation board. However, it has to be emphasized that the models were also validated with measurement results performed on a different evaluation board of the same commercial circuit. The low values of the NMSE suggest that the extracted models are valid for the commercial circuit, and not only for the particular evaluation board used in the experimental setup. In spite of the fact that the training and validation signals are quite dissimilar, it is evident that the models exhibit good generalization properties that mostly agree with the previously commented results. It is notable that starting from 15 coefficients, all the models perform nearly flat, although there is some deterioration in the NMSE of the model of [6] as the complexity increases, which can be related to a more difficult generalization when the number of coefficients is very high. In agreement with this matter, the good performance of the VBW model, which exhibits a radial structure, is remarkable. According to Fig. 2, it presents a complexity similar to that of the MP model, but with better accuracy. In the rest of the models, the evaluation again places RPV, SRPV, and EVBW in a better position compared to MP, GMP, and the model of [6], although the differences are reduced to a few tenths of dB.

In addition to the NMSE, another figure of merit for model performance assessment is the adjacent channel error power ratio (ACEPR), defined as the power of the error signal, calculated as the difference between the measured and modeled signal, in the adjacent channel relative to the power within the channel [14]. The ACEPR associated with the different models for the MAX2430 amplifier driven with OFDM signals is depicted in Fig. 7, where we observe results similar to those of the NMSE. In this case, starting from 15 coefficients, the best performance is for the RPV, with the SRPV following closely the curve. The rest of the models present similar performance.

The spectra of the measured and predicted signals are depicted in Fig. 8 for the case of cross-validation, i.e., the models were trained with OFDM excitations and the extracted kernels were subsequently tested with WCDMA signals. The traces in the upper part of the figure correspond to measurement data (dots) and the simulated spectra for the fifth-order RPV model with a memory length of four samples (solid line). Comparing with the GMP model of the same order and memory length, if we recall that the NMSE values attained in Fig. 6 were very low, it is not possible to distinguish the two traces from the measurements (only the RPV model is depicted). Likewise, the spectra of the error signals for the RPV and GMP models (solid line and dotted line in the lower part of Fig. 8) reveal comparable performance.

Finally, the set of measurements used for identification was also applied to a ZHL-5-2G amplifier (Minicircuits Inc., Brooklyn, NY), a 5-W PA useable over 700 to 2200 MHz operated with a dc voltage of 24 V, and using the same OFDM signal at a carrier frequency of 2 GHz. The excitation level was about 5 dB below the input 1-dB compression point. The performance in the spectral domain is compared again in Fig. 9. In this case, there are no significant differences, although the level of the error signal for the RPV model is lower in the signal channel. However, it is important to emphasize that this amplifier was driven at a more linear point

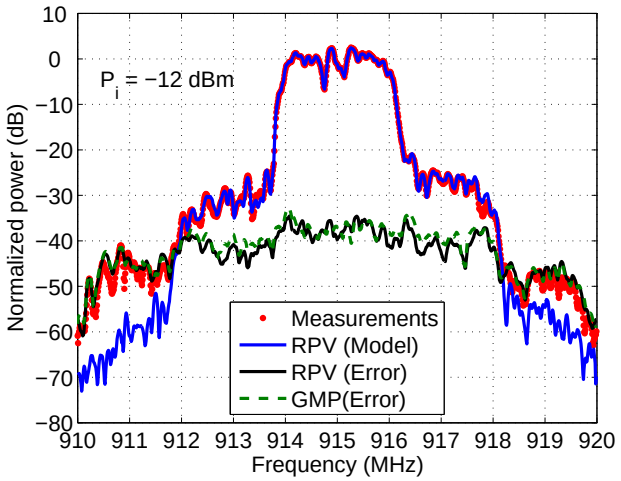


Fig. 8. Power spectra of the measured, modeled, and error signals simulated with fifth-order GMP and RPV models. Amplifier under test: MAX2430 excited by a 915-MHz WCDMA signal with 4-dB PAR, at a level of −12 dBm. Model identification was accomplished by using a 915-MHz OFDM test signal with 8 subcarriers and 8.4-dB PAR at the same level. Resolution bandwidth: 100 kHz.

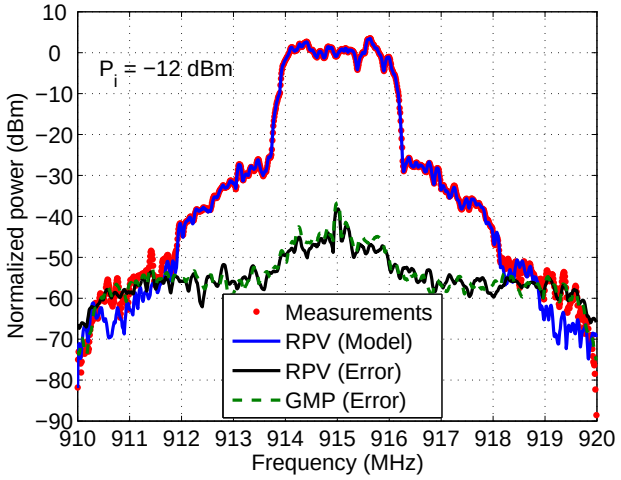


Fig. 9. Power spectra of the measured, modeled, and error signals simulated with fifth-order GMP and RPV models. Amplifier under test: ZHL-5-2G excited by a 2-GHz OFDM signal with 8 subcarriers and 8.4-dB PAR at a level of −12 dBm. Resolution bandwidth: 100 kHz.

of operation, compared to the MAX2430.

## VI. Conclusions

In this paper, we have presented a novel approach to prune discrete-time complex-baseband Volterra models by selecting radial directions. The proposed method accomplishes a significant reduction in the number of coefficients, with a complexity that compares favorably with that of other widely used behavioral models. The family of models has been extensively tested with measurement data from a class-AB amplifier at 915 MHz and a 5-W amplifier at 2 GHz. The obtained values of the NMSE were as low as −35 dB for a memory length of only two samples with a WCDMA signal at a strongly nonlinear point of operation, and near −33 dB for an OFDM signal with eight subcarriers when the input backoff was set at 5 dB. In this case the comparison in terms of the ACEPR showed that the proposed model obtained the best scores, with a value below −35 dB with two delay taps, which outperforms the other available models by about 1 dB. The computational cost of the models has been reduced due to the the radial pruning, which allows a trade-off between the number of parameters of the model and its accuracy. The good results place the proposed approach as a model of choice for behavioral modeling applied to predistortion techniques for PAs with memory.

Comparing the mathematical expression of the regressors defined for most of the Volterra-based behavioral models used for PAs, our results seem to show that the radial structure is relevant to the general configuration of a FV model. However, further work is necessary to demonstrate the physical origin of these radial terms, which could be derived from a circuit-level approach like that used to devise the VBW model in [5].

Another topic of interest is the improved performance that these models experience when even-order terms are included in the model definition [12]. As their origin is not due to any even-order term in the bandpass PA model, it is convenient to elucidate whether the associated improvement is due to compensation of baseband nonlinearities.

## Acknowledgment

The authors would like to thank the reviewers for their helpful suggestions and the quality of their comments.

## References

[1] J. Kim and K. Konstantinou, “Digital predistortion of wideband signals based on power amplifier model with memory,” *Electron. Lett.*, vol. 37, no. 23, pp. 1417-1418, Nov. 2001.

[2] A. Zhu and T. J. Brazil, “Behavioral modeling of RF power amplifiers based on pruned Volterra series,” *IEEE Microw. Wireless Compon. Lett.*, vol. 14, no. 12, pp. 563–565, Dec. 2004.

[3] A. Zhu, J. C. Pedro, and T. J. Brazil, “Dynamic deviation reduction-based Volterra behavioral modeling of RF power amplifiers,” *IEEE Trans. Microw. Theory Tech.*, vol. 54, no. 12, pp. 4323–4332, Dec. 2006.

[4] D. R. Morgan, Z. Ma, J. Kim, M. G. Zierdt, and J. Pastalan, “A generalized memory polynomial model for digital predistortion of RF power amplifiers,” *IEEE Trans. Signal Process.*, vol. 54, no. 10, pp. 3852–3860, Oct. 2006.

[5] C. Crespo-Cadenas, J. Reina-Tosina, and M. J. Madero-Ayora, “Volterra behavioral model for wideband RF amplifiers,” *IEEE Trans. Microw. Theory Tech.*, vol. 55, no. 3, pp. 449–457, Mar. 2007.

[6] D. Wisell and M. Isaksson, “Derivation of a behavioral RF power amplifier model with low normalized mean-square error,” in *Proc. 37th. European Microw. Conf.*, Munich, Germany, Oct. 2007, pp. 485–488.

[7] A. Zhu, J. C. Pedro, and T. R. Cunha, “Pruning the Volterra series for behavioral modeling of power amplifiers using physical knowledge,” *IEEE Trans. Microw. Theory Tech.*, vol. 55, no. 5, pp. 813–821, May 2007.

[8] O. Hammi, F. M. Ghannouchi, and B. Vassilakis, “A compact envelope-memory polynomial for RF transmitters modeling with application to baseband and RF-digital predistortion,” *IEEE Microw. Wireless Compon. Lett.*, vol. 18, no. 5, pp. 359–361, May 2008.

[9] C. Crespo-Cadenas, J. Reina-Tosina, and M. J. Madero-Ayora, “Performance of an extended behavioral model for wideband amplifiers,” in *IEEE 2008 Asia-Pacific Microw. Conf. Dig.*, Hong Kong, Dec. 2008. pp. 1–4.

[10] S. Chen, C. F. N. Cowan, and P. M. Grant, “Orthogonal least squares learning algorithm for radial basis function networks,” *IEEE Trans. Neural Networks*, vol. 2, no. 2, pp. 302–309, Mar. 1991.

[11] J. Tsimbinos and K. V. Lever, “Computational complexity of Volterra based nonlinear compensators,” *Electron. Lett.*, vol. 32, no. 9, pp. 852-854, Apr. 1996.

[12] L. Ding, and G. T. Zhou, "Effects of even-order nonlinear terms on power amplifier modeling and predistortion linearization," *IEEE Trans. Vehicular Technol.*, vol. 53, no. 1, pp. 156–162, Jan. 2004.
[13] A. Zhu, P. J. Draxler, J. J. Yan, T. B. Brazil, D. F. Kimball, and P. M. Asbeck, "Open-loop digital predistorter for RF power amplifiers using dynamic deviation reduction-based Volterra series," *IEEE Trans. Microw. Theory Tech.*, vol. 56, no. 7, pp. 1524–1534, Jul. 2008.
[14] M. Isaksson, D. Wisell and D. Ronnow, "Nonlinear behavioral modeling of power amplifiers using radial-basis function neural networks," in *IEEE MTT-S Int. Microwave Symp. Dig.*, Los Angeles, CA, 2006, pp. 1967–1970.

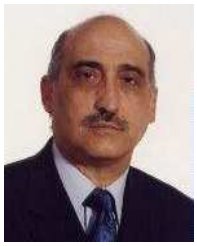

**Carlos Crespo-Cadenas** (A'94–M'09) was born in Madrid, Spain. He received the degree in Physics in 1973 and Doctor degree in 1995 from the Polytechnique University of Madrid. Since 1998 he has been Associate Professor and currently he teaches lectures on Radio Communications in the Department of Signal Theory and Communications, University of Seville. His current interests are Nonlinear Analysis applied to Wireless Digital Communications and to Microwave Monolithic Integrated Circuits (MMIC).

**Javier Reina-Tosina** (S'98–A'03–M'06) was born in Seville, Spain, in May 1973. He received the Telecommunication Engineering and Doctor degrees from the University of Seville, Seville, Spain, in 1996 and 2003, respectively. Since 1997 he has been with the Department of Signal Theory and Communications, University of Seville, where he is currently an Associate Professor. His research interests include MMIC technology, nonlinear analysis of active microwave devices and integration of information technologies in biomedicine.

**María J. Madero-Ayora** (S'06–M'09) received the Telecommunication Engineering and Doctor degrees from the University of Seville, Seville, Spain, in 2002 and 2008, respectively. Since 2003 she has been with the Department of Signal Theory and Communications, University of Seville, and is currently Assistant Professor. Her research interests focus on the area of nonlinear analysis of active microwave devices and measurement techniques for nonlinear communication systems.